CHEMISTRY
A EUROPEAN JOURNAL

DOI: 10.1002/chem.201101861

Cycloalkane and Alicyclic Heterocycle Complexation by New Switchable Resorcin[4]arene-Based Container Molecules: NMR and ITC Binding Studies**

Jens Hornung,[a] Daniel Fankhauser,[a] Laura D. Shirtcliff,[a, b] Antonia Praetorius,[a] W. Bernd Schweizer,[a] and François Diederich*[a]

Abstract: The synthesis and structural characterization of novel, "molecular basket"-type bridged cavitands is reported. The resorcin[4]arene-based container molecules feature well-defined cavities that bind a wide variety of cycloalkanes and alicyclic heterocycles. Association constants (K_a) of the 1:1 inclusion complexes were determined by both ^{1}H NMR and isothermal titration calorimetry (ITC). The obtained K_a values in mesitylene ranged from $1.7\times10^2\,M^{-1}$ for cycloheptane up to $1.7\times10^7\,M^{-1}$ for morpholine. Host–guest complexation by the molecular baskets is generally driven by dispersion interactions, C–H···π interactions of the guests with the aromatic walls of the cavity, and optimal cavity filling. Correlations between NMR-based structural data and binding affinities support that the complexed heterocyclic guests undergo additional polar C–O···C=O, N–H···π, and S···π interactions. The first crystal structure of a cavitand-based molecular basket is reported, providing precise information on the geometry and volume of the inner cavity in the solid state. Molecular dynamic (MD) simulations provided information on the size and conformational preorganization of the cavity in the presence of encapsulated guests. The strongest binding of heterocyclic guests, engaging in polar interactions with the host, was observed at a cavity filling volume of 63 ± 9 %.

Keywords: container molecules · controllable encapsulation · host–guest systems · molecular recognition · supramolecular chemistry

Introduction

Bridged resorcin[4]arene-derived container molecules ("molecular baskets") feature two diazaphthalimide side walls connected by a rigid bridge in an *anti*-orientation and two flexible quinoxaline flaps. These container molecules undergo a switchable conformational change from a closed *vase* to an open *kite* form by modulation of pH or temperature (Figure 1).[1,2]

In the *vase* form, the inner cavity of the bridged resorcin[4]arene-derived cavitands is completely enclosed, allowing stable host–guest complexation in solution.[1,2] In comparison to the original, open-top cavitands with four identical quinoxaline flaps introduced and studied by Cram and coworkers[3,4] as well as by others,[5–7] the acid (CF_3COOH (TFA)) concentration required for complete *vase*-to-*kite* switching of the bridged cavitands is higher by one order of magnitude.[2] The bridge spanning the diazaphthalimide side walls enforces and rigidifies the *vase* conformation of the cavitand, which increases host–guest binding strength.[2] Open, rim-decorated resorcin[4]arene cavitands have also been shown to form stable inclusion complexes;[8–10] however, their conformational flexibility remains high,[10] which limits precise molecular recognition studies in the interior cavity.

Here, we present the syntheses and properties of two new switchable cavitands (**1** and **2** in Figure 2) with rigidifying *para*-xylylene bridges and different legs. The first crystal structure of a cavitand-based molecular basket is reported, providing precise information on the geometry and volume of the inner cavity in the solid state. Host–guest studies using cavitand **1** and a wide variety of alicyclic and alicyclic heterocyclic compounds were performed by ^{1}H NMR and isothermal titration calorimetry (ITC) to determine the K_a values of the formed inclusion complexes and to decipher the interactions between bridged cavitand and guest molecule. Heterocycles were of particular interest for exploration of polar interactions between the complexed guests and the surrounding host molecule. This study therefore comple-

[a] Dr. J. Hornung,[+] D. Fankhauser,[+] Dr. L. D. Shirtcliff, A. Praetorius, Dr. W. B. Schweizer, Prof. F. Diederich
Laboratorium für Organische Chemie, ETH Zürich
Hönggerberg, HCI, CH-8093 Zürich (Switzerland)
Fax: (+41) 44-632-1109
E-mail: diederich@org.chem.ethz.ch

[b] Dr. L. D. Shirtcliff
Current address: Department of Chemistry
Oklahoma State University
107 Physical Science, Stillwater, OK 74074 (USA)

[+] Contributed equally to this work.

[**] ITC = Isothermal Titration Calorimetry.

Supporting information for this article is available on the WWW under http://dx.doi.org/10.1002/chem.201101861.

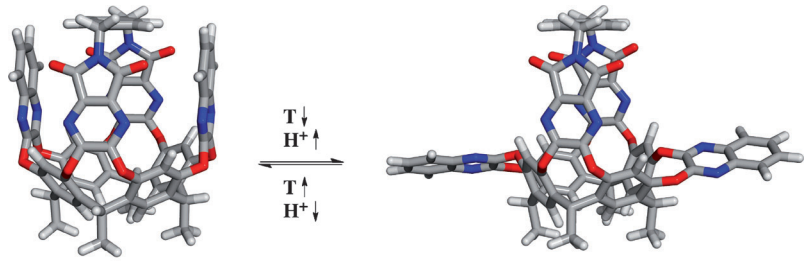

Figure 1. Conformational *vase–kite* switching of a molecular basket-type container molecule.

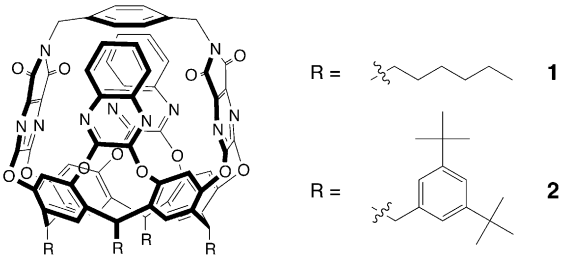

Figure 2. Structures of the bridged cavitands **1** and **2**.

ments the previous investigations on apolar binding processes inside container molecules by Mecozzi and Rebek.[11]

Results and Discussion

Synthesis: The syntheses of molecular baskets **1** and **2** are outlined in Scheme 1. Aldehyde **3** was synthesized in three steps from commercially available 3,5-di-*tert*-butyltoluene, avoiding previously used cyanide chemistry and improving the overall yield from 25% to 42% compared to literature procedures.[12,13] Aldehyde **4**[14] was subjected to a Wittig reaction, affording a mixture of *cis*- and *trans*-vinyl methyl ethers **5a** and **5b**. The two isomers were isolated and characterized separately, but reacted together in the next step to afford aldehyde **3**. Condensation of resorcinol with aldehyde **3**, following standard procedures, afforded octol **6** in 33% yield.[15] Bridging of **6** with 2,3-dichloroquinoxaline afforded cavitand **7**[12–16] from which two bridges were selectively removed to afford *anti*-tetrol **8** (Scheme 1A).[13,17,18]

In contrast to our previously published work,[1,2] the basket bridge was introduced in one single step. For this transformation, the bis(dichlorodiazaphthalimide) **9** was prepared by condensation of anhydride **10**[17] and the HCl salt of commercially available 1,4-bis(aminomethyl)benzene (Scheme 1A).

Bridging moiety **9** was subsequently allowed to react with tetrol **8** under basic conditions to afford cavitand **2** in 6% isolated yield. In addition, the tube-type dimeric **11** was obtained in 9% yield (Scheme 1B). Similarly, cavitand **1** was synthesized in 23% isolated yield by reacting **9** with the known tetrol **12** bearing *n*-hexyl legs.[13,18] Additionally, dimeric **13** was obtained in 10% yield (Scheme 1B). The spectroscopic properties fully support the molecular structures assigned to **1**, **2**, **11**, and **13**, which are stable, colorless solids, decomposing around 300°C (for the binding and switching properties of tube **13**, see Figure 1SI and 2SI in the Supporting Information).

X-ray crystal structure of molecular basket 2: A crystal structure for an open cavitand with four quinoxaline walls and di-*tert*-butylbenzyl legs was published in 2001 by our group.[15] Crystals suitable for X-ray analysis were obtained from a solution of **2** in CH_2Cl_2/heptane by slow evaporation of CH_2Cl_2. The crystal structure (space group: monoclinic $P2_1$) shows the cavitand in the *vase* conformation (Figure 3). Strong disordering of atoms in the di-*tert*-butylbenzyl legs, which was observed in our earlier published structure as well,[15] rendered the location and refinement of individual atom positions of some of the leg atoms impossible. The structure from the X-ray experiment showed a well-defined cavity, two complete di-*tert*-butylbenzyl legs and a part of a third one. The completely disordered atoms of two of the di-*tert*-butylbenzyl residues could not be resolved and were therefore calculated and refined as rigid body allowing the *tert*-butyl groups to rotate.

The guest molecule inside the cavity could be a CH_2Cl_2 molecule with the two chlorines aligned almost on an axis passing through the phenyl ring of the bridge and the center of the rim, positioned below and above the level of the quinoxaline N atoms. The CH_2Cl_2 carbon is fully disordered in the crystal and could not be seen; the distance of 2.87 Å between the two Cl atoms suggests the presence of a CH_2Cl_2 molecule (Cl–Cl distance: 2.843 Å).[19] However, some uncertainty remains, as the resolution of the guest is rather low. The crystal packing shows a head-to-tail arrangement forming infinite columns along the *a* axis (see Figure 3SI). The neighboring columns have an antiparallel orientation towards each other. We assume that the low resolution of the crystal structure results from disorder, most probably caused by a rotation of the molecules by 90° along the stacking axes.

Host–guest studies by ^{1}H NMR spectroscopy and ITC: Complexation studies by ^{1}H NMR spectroscopy and ITC with the more soluble basket **1** were carried out in mesitylene at 303 K. Mesitylene is the solvent of choice as it does not fit inside the cavity and therefore cannot compete for binding.[7,20,21] However, molecular basket cavitands have been shown to bind minute solvent impurities. Therefore, the purities of commercially available deuterated and non-deuterated mesitylene were examined by GC/MS. In [D_{12}]mesitylene, deuterated impurities were found. These impurities are invisible in the ^{1}H NMR spectra but potentially compete with the investigated guests for interior bind-

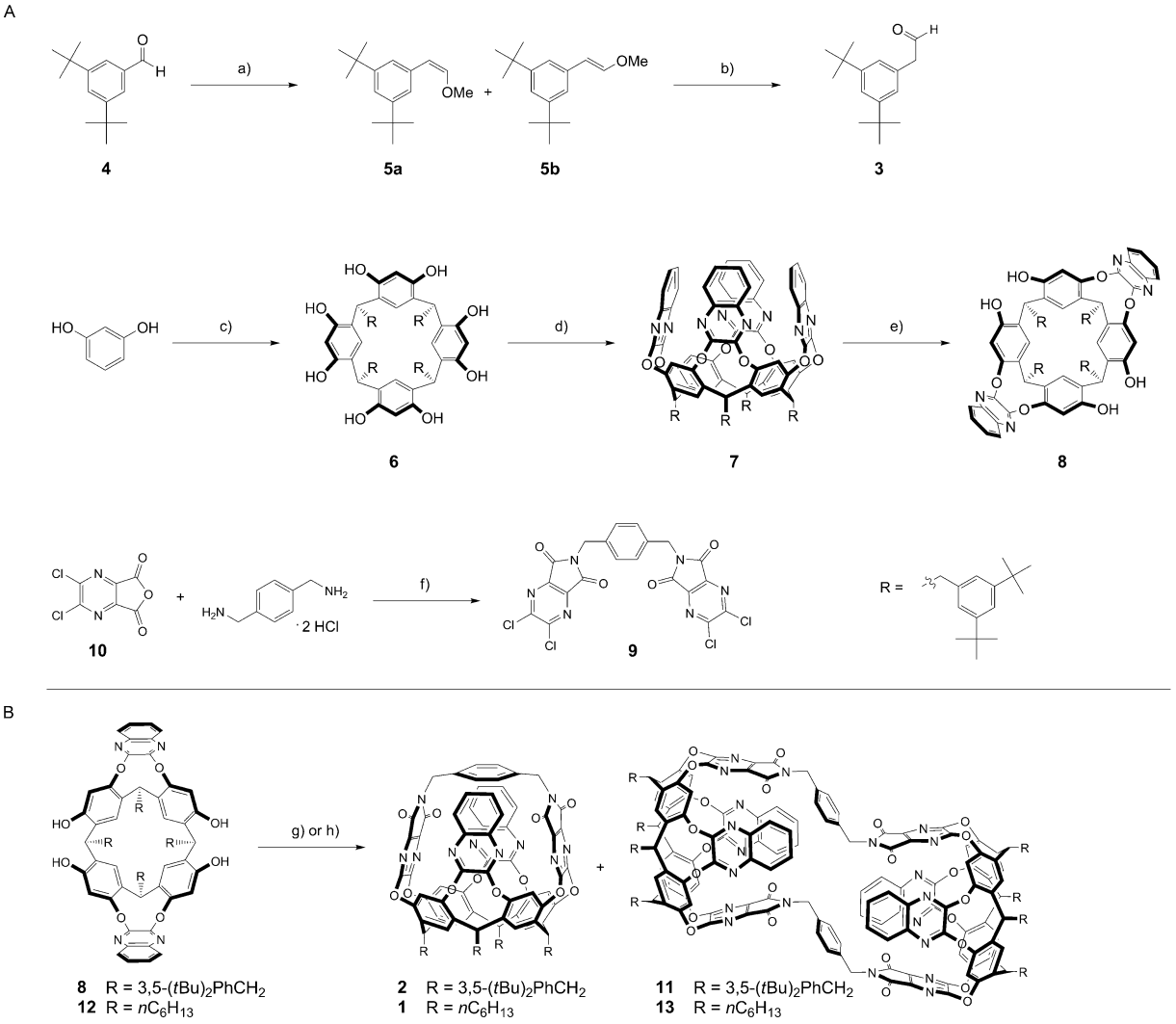

Scheme 1. Synthesis of molecular baskets **1** and **2**. a) $(C_6H_5)_3P^+CH_2OCH_3\ Cl^-$, NaH, THF, 18 h, reflux; 80% (**5a**), (**5b**). b) HCOOH, CH_2Cl_2, 20 h, 25°C; 69%. c) **3**, HCl, EtOH, 5 days, 60°C; 33%. d) 2,3-Dichloroquinoxaline, K_2CO_3, DMF, 48 h, 60°C; 80%. e) CsF, catechol, DMF, 1 h, 80°C; 46%. f) Ac_2O, sealed tube, 80 min, 125°C; 68%. g) **9**, Et_3N, DMF, 18 h, 70°C; 6% (**2**), 9% (**11**); h) **9**, DIPEA, DMF, 18 h, 85°C; 23% (**1**), 10% (**13**). DIPEA = diisopropylethylamine; DMF = *N*,*N*-dimethylformamide.

ing. By careful distillation, realized by the vendor, high-quality $[D_{12}]$mesitylene was obtained (see Figure 4SI). The only remaining, very minor impurities are non-separable, deuterated structural isomers of $[D_{12}]$mesitylene, which could possibly fit inside the cavity and compete with guests.

A variety of cycloalkanes and alicyclic heterocycles of different sizes were chosen as guests (Figure 4). In addition, we attempted to investigate azetane, glutarimide, and morpholin-3-one. All three substances, however, were not sufficiently soluble in mesitylene to accurately determine association constants.

Molecular basket host–guest exchange kinetics are slow on the ^{1}H NMR time scale at 303 K, and K_a values can be determined from the ratio of the signals of free and encapsulated guest, with the latter appearing in the δ range beween −2 and −4 ppm. Due to the fact that a large number of free guest resonances appear in the area of the hexyl resonances of host **1**, a proper determination of the free guest peak area was problematic. We overcame this problem by using an internal standard (1,3,5-trimethoxybenzene) and evaluated the peak area of encapsulated guest signals against this standard. 1,3,5-Trimethoxybenzene is not a competitive binder and has no overlapping ^{1}H NMR signals. ^{1}H NMR signals for all unbound guests in $[D_{12}]$mesitylene and for the bound guests that were analyzed by this method are listed in Table 1SI.

^{1}H NMR measurements of host **1** in $CDCl_3$ indicated the presence of a single host species, presumably forming a 1:1 host–guest complex with $CDCl_3$. In $[D_{12}]$mesitylene, however, three different sets of host signals were observed. We speculate that the deuterated structural isomers of $[D_{12}]$mesitylene, which were found by GC/MS, possible fit in the cavity and therefore produce different signals. When the sample was heated to 423 K, only one set of signals was

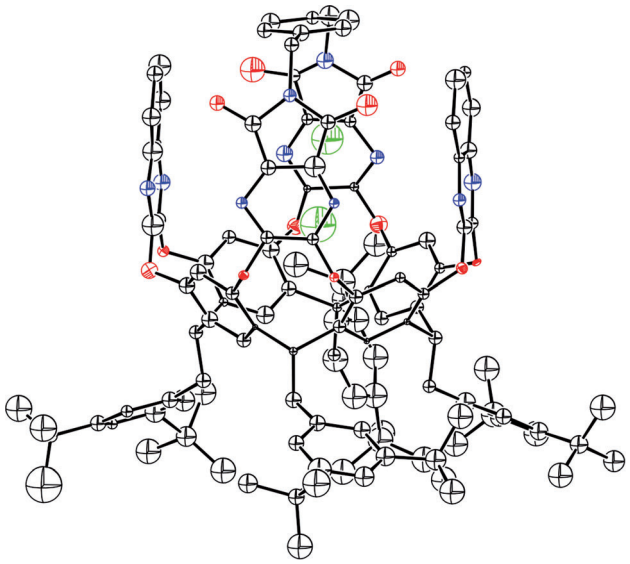

Figure 3. Crystal structure of molecular basket **2** at 100 K. Atoms are shown with isotropic temperature factors at the 50% level.

present (Figure 5SI), as complexation/decomplexation becomes fast on the ^{1}H NMR time scale. Additionally, after addition of any guest (>1 equiv) at 303 K, one set of host signals was observed as well. In this case, all signals of the host–guest complex could be readily assigned. As an example, the ^{1}H NMR spectrum of host **1** with encapsulated morpholine (1.2 equiv) as guest (298 K, [D_{12}]mesitylene) is shown in Figure 6SI.

With ^{1}H NMR spectroscopy, association constants can only be accurately determined in the range of 10–10^4 M^{-1}.[22] ITC analysis, however can accurately determine association constants between 10^4–10^7 M^{-1}.[23] Determination of K_a values above 10^4 M^{-1} by ^{1}H NMR spectroscopy is limited by the accuracy of the measured integrals, while the small evolution of heat for encapsulation of guests with K_a values below 10^4 M^{-1} prevents accurate ITC analysis. The results of ^{1}H NMR spectroscopic and ITC binding studies with host **1** are summarized in Table 1.[24] Preliminary binding studies with tube **13** are reported in the Supporting Information (Figure 1SI).

Results for the complexation of cyclohexane and thietane obtained by both methods were reproducible and comparable among each other. However, K_a values from NMR data were slightly smaller than from ITC measurements. This is most likely due to the higher purity of the non-deuterated mesitylene, as compared to the deuterated one: in the deuterated solvent, more solvent impurities compete with the guest for the cavity binding site.

Guest exchange can be monitored by guest competition experiments. This is shown in Figure 7SI for the displace-

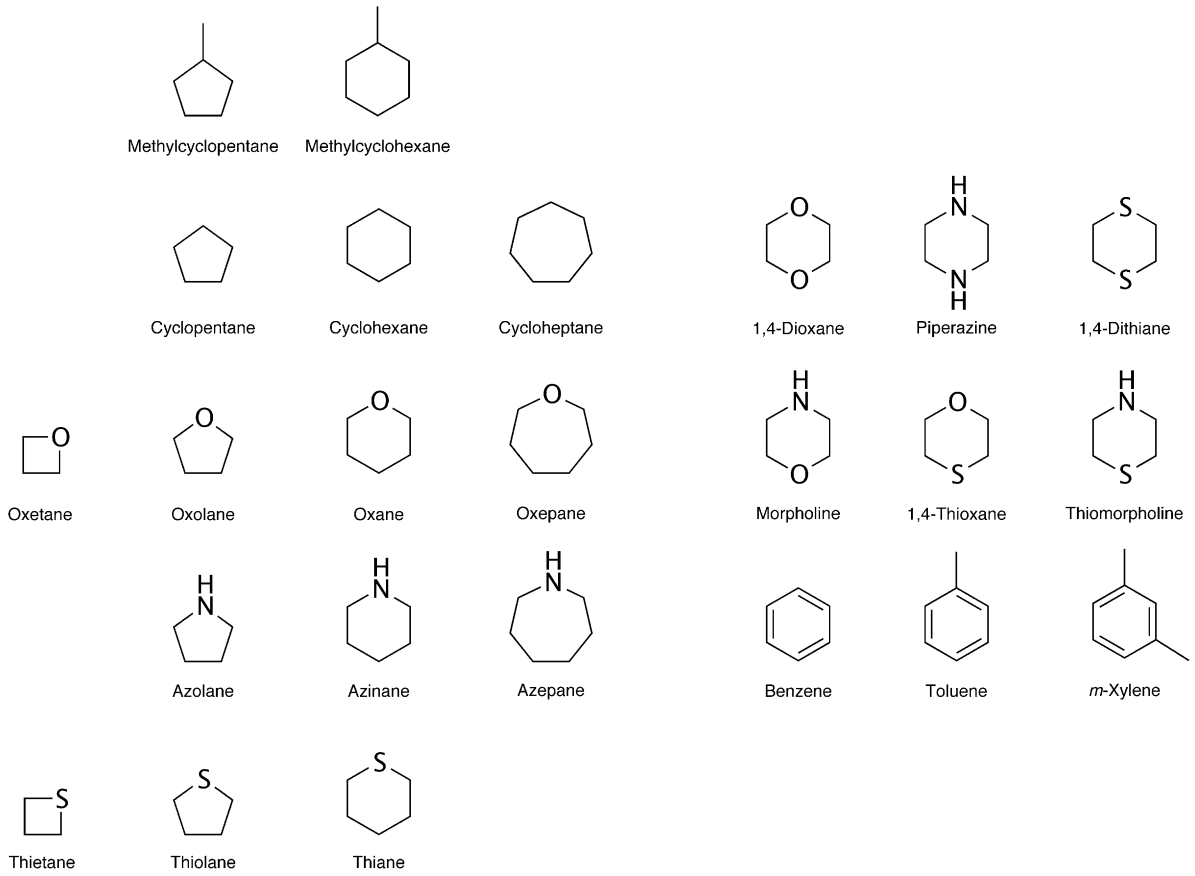

Figure 4. Structures of guest molecules used in binding studies.

Table 1. Host–guest complexes with 1:1 stoichiometry formed by molecular basket **1** in mesitylene (ITC) and [D_{12}]mesitylene (^{1}H NMR spectroscopy) at 303 K. The volumes of free guest and the host cavities in the complexes, packing coefficients, and thermodynamic data determined by ITC analysis and ^{1}H NMR spectroscopy are shown.

Complex	V_{Guest} [Å^3]	V_{Cavity} [Å^3][f]	PC_{MD}	K_a [M^{-1}][a]	ΔH [kJ mol^{-1}]	ΔS [J mol^{-1}K^{-1}]	ΔG [kJ mol^{-1}][g]	K_a [M^{-1}][b]
methylcyclopentane ⊂ **1**	102.3	155.1 ± 9.1	0.66 ± 0.04	–[c]	–[c]	–[c]	–[c]	(1.5 ± 0.2) × 10^3
methylcyclohexane ⊂ **1**	118.5	172.8 ± 9.6[h]	0.69 ± 0.04	–[e]	–[e]	–[e]	–[e]	–[e]
cyclopentane ⊂ **1**	85.2	141.2 ± 5.9	0.60 ± 0.03	(1.2 ± 0.1) × 10^5	−13.8 ± 0.2	51.5 ± 1.5	−29.4 ± 0.3	–[d]
cyclohexane ⊂ **1**	101.9	146.7 ± 5.9	0.69 ± 0.03	(2.3 ± 0.5) × 10^4	−12.8 ± 0.7	41.2 ± 3.8	−25.2 ± 0.6	(3.0 ± 0.8) × 10^3
cycloheptane ⊂ **1**	117.6	157.1 ± 8.3	0.75 ± 0.04	–[c]	–[c]	–[c]	–[c]	(1.7 ± 0.1) × 10^2
oxetane ⊂ **1**	62.0	139.6 ± 6.5	0.44 ± 0.02	–[c]	–[c]	–[c]	–[c]	(4.6 ± 0.1) × 10^3
oxolane ⊂ **1**	77.2	140.0 ± 5.9	0.55 ± 0.02	(3.2 ± 1.5) × 10^5	−9.4 ± 0.5	73.5 ± 6.1	−31.6 ± 1.3	–[d]
oxane ⊂ **1**	93.6	142.8 ± 6.0	0.66 ± 0.03	(1.5 ± 0.1) × 10^6	−21.4 ± 0.3	47.9 ± 1.0	−35.9 ± 0.1	–[d]
oxepane ⊂ **1**	109.7	151.8 ± 7.0	0.72 ± 0.03	(2.5 ± 0.5) × 10^5	−21.6 ± 1.9	31.7 ± 8.1	−31.2 ± 0.6	–[d]
azolane ⊂ **1**	80.2	139.9 ± 6.0	0.57 ± 0.02	(8.0 ± 1.9) × 10^5	−11.9 ± 0.2	73.8 ± 3.2	−34.2 ± 0.6	–[d]
azinane ⊂ **1**	98.0	142.9 ± 5.9	0.69 ± 0.03	(2.4 ± 0.2) × 10^6	−24.2 ± 0.3	42.2 ± 1.8	−37.0 ± 0.2	–[d]
azepane ⊂ **1**	114.3	152.1 ± 7.5	0.75 ± 0.04	–[i]	–[i]	–[i]	–[i]	(1.8 ± 1.0) × 10^5
thietane ⊂ **1**	70.9	139.5 ± 6.1	0.51 ± 0.02	(4.2 ± 0.1) × 10^4	−8.8 ± 0.1	59.7 ± 0.1	−26.9 ± 0.1	(3.9 ± 1.2) × 10^4
thiolane ⊂ **1**	87.7	140.6 ± 6.1	0.62 ± 0.03	(1.6 ± 0.1) × 10^6	−17.4 ± 0.4	61.5 ± 1.8	−36.0 ± 0.1	–[d]
thiane ⊂ **1**	103.5	148.6 ± 6.8	0.70 ± 0.03	(1.3 ± 0.1) × 10^5	−13.5 ± 0.4	53.6 ± 1.8	−29.7 ± 0.1	–[d]
1,4-dioxane ⊂ **1**	85.4	142.9 ± 6.1	0.60 ± 0.03	(1.1 ± 0.4) × 10^7	−21.8 ± 2.2	62.5 ± 3.1	−40.7 ± 1.0	–[d]
piperazine ⊂ **1**	94.3	143.5 ± 6.5	0.66 ± 0.03	(8.5 ± 0.6) × 10^6	−23.8 ± 0.4	54.4 ± 2.1	−40.2 ± 0.2	–[d]
1,4-dithiane ⊂ **1**	104.8	150.9 ± 7.2	0.69 ± 0.03	(3.3 ± 0.1) × 10^5	−16.8 ± 0.1	50.3 ± 0.1	−32.1 ± 0.1	–[d]
morpholine ⊂ **1**	89.5	142.5 ± 5.8	0.63 ± 0.03	(1.7 ± 0.4) × 10^7	−24.6 ± 0.5	57.0 ± 5.0	−41.8 ± 0.7	–[d]
1,4-thioxane ⊂ **1**	98.4	144.9 ± 6.3	0.68 ± 0.03	(3.2 ± 0.2) × 10^6	−19.1 ± 0.1	61.5 ± 0.1	−37.8 ± 0.1	–[d]
thiomorpholine ⊂ **1**	98.4	145.5 ± 6.2	0.68 ± 0.03	(3.5 ± 0.2) × 10^6	−22.2 ± 0.5	52.2 ± 2.0	−38.0 ± 0.1	–[d]
benzene ⊂ **1**	82.4	145.0 ± 7.3	0.57 ± 0.03	(9.7 ± 0.6) × 10^5	−14.1 ± 0.1	68.2 ± 0.9	−34.7 ± 0.2	–[d]
toluene ⊂ **1**	97.0	165.6 ± 17.9[h]	0.59 ± 0.06	–[c]	–[c]	–[c]	–[c]	(2.5 ± 0.6) × 10^3
m-xylene ⊂ **1**	117.2	186.8 ± 11.3[h]	0.63 ± 0.04	–[c]	–[c]	–[c]	–[c]	(2.2 ± 0.3) × 10^2

[a] K_a values determined by ITC (double to pentuple runs). [b] K_a values determined by ^{1}H NMR spectroscopy (double to quadruple runs). [c] Evolution of heat was too small for determination of an association constant by ITC. [d] K_a values are too high for determination by ^{1}H NMR spectroscopy. [e] No binding was observed. [f] Determined by MD calculations according to the literature.[2] [g] Calculated with $\Delta G = -RT\ln K_a$. [h] Calculation was not convergent. [i] Calculation not possible due to impossible curve fitting.

ment of the weaker guest cycloheptane by the stronger-binding morpholine, waiting approximately 15 min after addition of the second guest before recording a new spectrum.

The detailed protocol for the ITC measurements is given in the Experimental Section. Selected ITC isotherms for titrations of a strongly binding guest (morpholine) and a weaker binder (cyclohexane) are shown in Figures 8SI–11SI. The full set of thermodynamic parameters obtained by ITC is included in Table 1. The stoichiometry of the host–guest complexes was determined by ITC to be 1:1 for all guests included in this study.

A comparison of the measured association constants shows that the most stable complexes (K_a values = 10^6 to 10^7 M^{-1}) are predominantly formed by alicyclic six-membered heterocycles. In comparison, the hydrocarbon cyclohexane only gives $K_a = 2.3 \times 10^4$ M^{-1}. Binding affinity of the heterocycles drops strongly into the range of $K_a = 10^3$–10^4 M^{-1} by either increasing or decreasing the ring size. Optimal volume occupancy (see below), dispersion interactions, and in particular C–H···π interactions between the encapsulated guest and the π surfaces in the walls, the resorcinarene bowl, and the cap of the host clearly are major contributors to the complexation strength. Compared to cyclic hydrocarbons, heterocyclic guests undergo stronger C–H···π interactions as a result of the higher polarization of the C–H bonds by the σ-withdrawing heteroatoms. This alone, however, cannot explain the large preference of host **1** for heterocyclic guests over hydrocarbon guests.

The thermodynamic parameters calculated from the experimental ITC data show that binding of all guests is promoted by both a favorable negative enthalpic term ΔH and a favorable positive entropic term ΔS (Table 1). The origins of the entropic driving force can be rationalized by the following points: i) The container is rigid and preorganized, and guest complexation does not substantially restrict its conformational mobility; ii) the favorable entropy of binding results from the empty host cavity in mesitylene, which is filled by the guest under gain of entropy of mixing;[1] iii) the unbound heterocyclic guests in the bulk mesitylene solvent might not have full freedom of rotation and translation. Rather, they might adopt preferred, more ordered alignments (as is known for molecules dissolved in benzene and reflected in the aromatic-solvent-induced shifts (ASIS))[25] so that electronegative oxygen atoms avoid pointing into the π surface; iv) guests with an H-bond donor and acceptor, such as morpholine, undergo intermolecular association in the apolar solvent.

An informative summary[26] of the results from the ITC analysis is documented in Figure 5. It shows that the gain in binding entropy is larger for smaller guests than for larger guests. Smaller guests lose less translational and rotational degrees of freedom upon complexation as they can still

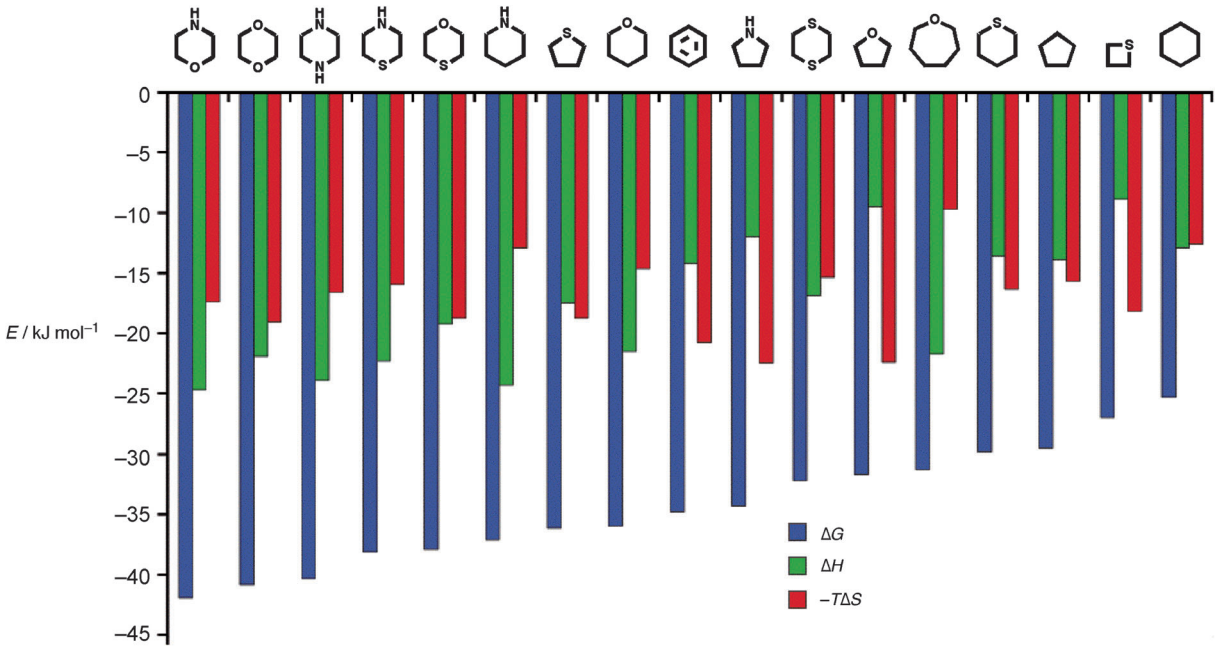

Figure 5. Thermodynamic quantities from ITC analysis at 303 K.

move inside the cavity. Accordingly, the enthalpic gain upon their inclusion is small, as tight contacts are not established (see azolane, oxolane, thietane).

Six-membered heterocycles are clearly among the most potent binders. While entropic gains for their encapsulation are less than in the case of the smaller analogs, they benefit from a particularly favorable complexation enthalpy. The complexation enthalpy for N,O-containing six-membered guests is uniformly below $\Delta H < -20\,\mathrm{kJ\,mol^{-1}}$, with morpholine topping the series at $\Delta H = -24.6\,\mathrm{kJ\,mol^{-1}}$, whereas cyclohexane only binds with $\Delta H = -12.8\,\mathrm{kJ\,mol^{-1}}$. We therefore analyzed which additional favorable interactions the various heterocyclic guests could undergo with the surrounding cavity walls.[2,27] To find the preferred orientation of the heteroatoms inside the cavity, rotating frame Overhauser effect spectroscopy (ROESY) experiments were performed (for examples, see Figure 12SI). We observed that the oxygen atoms in cyclic ethers (oxetane, oxolane, oxane, oxepane) point away from the electron-rich bowl towards the upper part of the container. We explain this orientational preference with additional favorable, near-orthogonal dipolar C–O···C=O interactions between the guests and the diazaphthalimide C=O groups.[28] According to computer modeling, repulsive contacts of the O atom with the *para*-xylylene bridge are avoided. The same observation was made with cyclic amines (azolane, azinane, azepane). When pointing towards the *para*-xylylene bridge, their N–H groups may undergo stabilizing N–H···π interactions.[29,30] Hydrogen bonding to the C=O groups in the container walls is geometrically not possible.

Sulfur-containing guests (thietane, thiolane, thiane) also point with their S atom towards the *para*-xylylene bridge, presumably to gain favorable S···π interactions.[30] In the complexes of morpholine and 1,4-thioxane, the oxygen of the guest points towards the upper part of the container; an orientation also adopted by the N–H moiety of thiomorpholine. It is therefore reasonable to suggest that additional polar contacts, such as orthogonal C–O···C=O, N–H···π, and S···π interactions stabilize the complexes of heterocyclic guests (Figure 6).[31] This is particularly reflected for six-membered heterocyclic guests in the highly favorable values for the complexation enthalpy ΔH and ultimately the complexation free enthalpy ΔG.

In comparison with previous host–guest studies from our group in less pure [D_{12}]mesitylene, containing among others 0.26% *m*-xylene, we found that K_a values and hence ΔG values are robust. However, our ΔH and ΔS values deter-

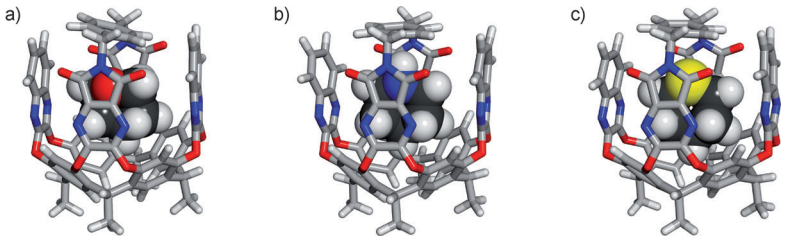

Figure 6. Preferred encapsulation geometries of oxane (a), azinane (b), and thiane (c), supported by ROESY experiments. Shown are the lowest-energy conformations of the complexes calculated using MacroModel 9.7 (OPLS 2005 force field, GB/SA solvation model for $CHCl_3$).

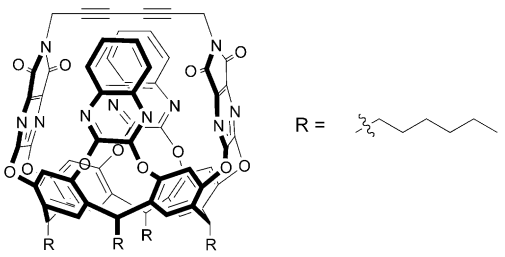

14

Figure 7. Structure of bridged cavitand **14**, which was synthesized and investigated in previous studies.[2]

mined previously from van't Hoff plots (VT-NMR spectroscopy) are not reliable.[2] This can be attributed to the fact that cavitand-based molecular baskets are notorious for their propensity to encapsulate even minor solvent impurities. These conclusions were derived by performing additional ITC studies with molecular basket **14**[2] in mesitylene of better quality (Figure 7). The suitability of van't Hoff analysis by VT-NMR spectroscopy for the determination of thermodynamic quantities for host–guest complexation by dynamic container molecules will require further investigation.

Cavity occupancy by guest molecules: Based on the X-ray crystal structure, the free-cavity volume in **2** (and therefore also in **1**) was determined to be 135 Å^3. We have previously shown in molecular dynamics simulations that molecular baskets adapt their cavity size to the guest ("induced fit") to optimize the fraction of occupied space.[2] For optimal accommodation of a smaller guest, the cavity volume contracts, as compared to the "static" volume seen in the crystal structure, while it expands to accept larger guests. We proposed that molecular dynamics simulations provide an appropriate way for determining packing coefficients PC, that is, the ratio of guest volume to host volume.[11] All host–guest complexes were submitted to molecular dynamics simulations using MacroModel 9.7 (OPLS 2005 force field, GB/SA solvation model for $CHCl_3$, 300 K, 1000 ps simulation time with 1.5 fs time steps).[32] The *n*-hexyl legs were substituted with methyl legs for the calculations. A total of 1000 geometries from each of the resulting trajectories were obtained for the host–guest complex, the guest was removed, and the empty host structures submitted to the program VOIDOO to determine the average cavity volumes.[33,34] Figure 13SI shows the VOIDOO cavity volume calculations for different host–guest complexes. Taking these volumes and those of the guests (geometry optimization using PM3 in SPARTAN[19] and subsequent volume determination by VOIDOO), the PC values shown in Table 1 were calculated.

In the series of alicyclic heterocycles, the best binding is established at a filling of about 63 ± 9% (Figure 8). This value is significantly higher than the value of 55 ± 9% published by Mecozzi and Rebek for the binding of liphophilic guests in apolar hosts, which is driven mainly by van der Waals interactions.[11] The Mecozzi–Rebek rule has held true

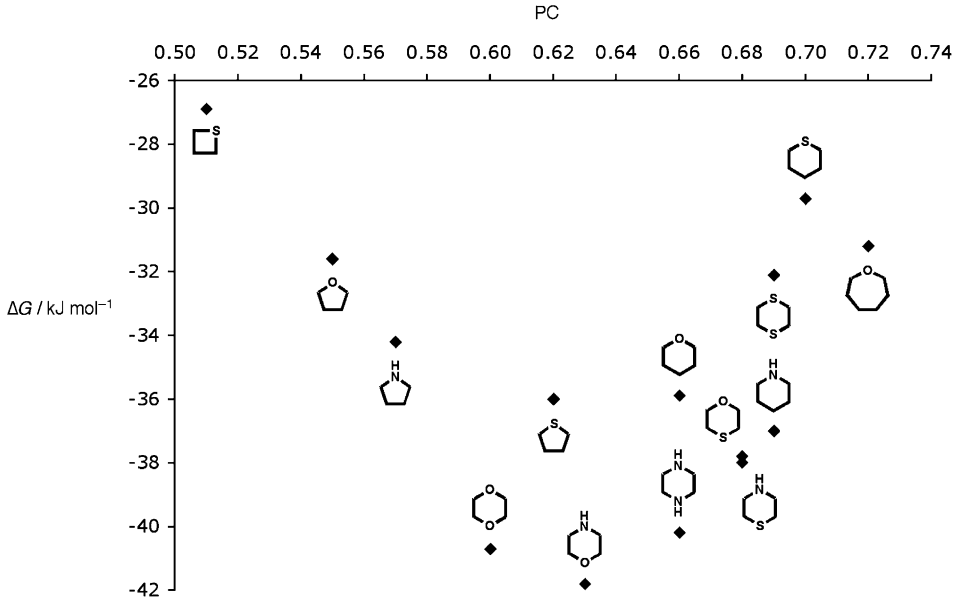

Figure 8. Diagram showing the free enthalpy for the binding of heterocycles vs. the PC (the ratio of guest volume to host volume)[11] of the corresponding inclusion complexes.

in studies of other apolar complexation processes in both chemistry and biology.[35,36] We suggest that the increase in the optimal PC in our series of complexes is due to the additional close polar contacts (C–O···C=O, N–H···π, and S···π) established in the complexes of host **1** with heterocyclic guests. As already mentioned by Rebek and Mecozzi,[11] the optimal PC increases when polar contacts are established in confined environments.

Conformational switching: One of the remarkable properties of the cavitand based molecular baskets is the ability to reversibly change their conformation upon pH modulation.[1,2] CF_3COOD protonates the mildly basic nitrogen atoms of the quinoxaline flaps, resulting in electrostatic repulsion and a change from *vase* to *kite* conformation, as illustrated in Figure 1. While complete *vase*-to-*kite* switching of open cavitands with four quinoxaline walls occurs at $[CF_3COOD] \approx 0.4$ M, bridged cavitands require a much higher concentration of acid.

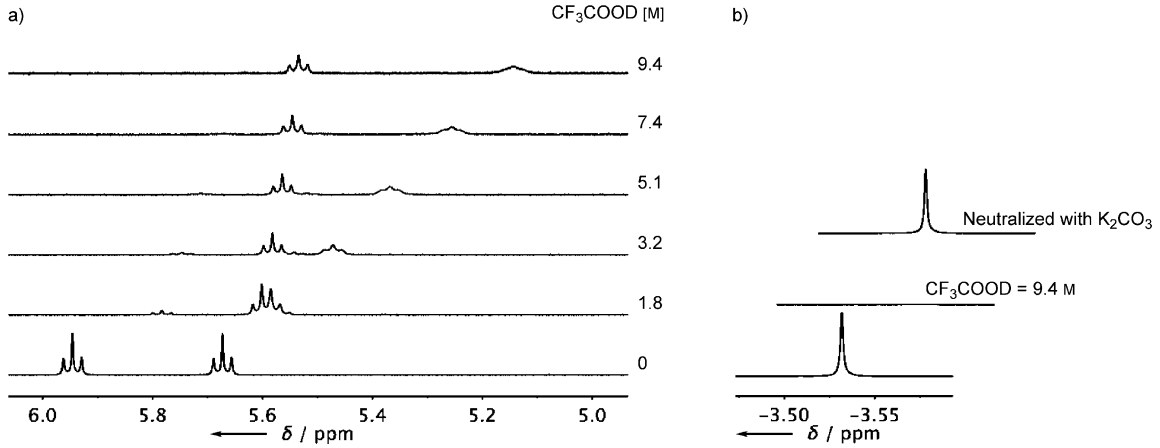

Figure 9. a) Acid-induced *vase–kite* switching of cavitand **1** (2.9×10^{-3} M) with cyclopentane encapsulated (1.2 equiv) monitored by ^{1}H NMR spectroscopy (500 MHz, [D_{12}]mesitylene, 303 K). b) Cutout from ^{1}H NMR spectra (500 MHz, [D_{12}]mesitylene, 303 K) of cyclopentane (1.2 equiv) encapsulated in **1** (2.9×10^{-3} M), upon acidification by CF_3COOD and after neutralization with aqueous K_2CO_3. The dilution of the host–guest complex based on the experiment is mathematically corrected.

The ^{1}H NMR spectra for the H^+-induced switching process of bridged cavitand **1** (2.9×10^{-3} M) with encapsulated cyclopentane (1.2 equiv) in [D_{12}]mesitylene at 303 K is outlined in Figure 9. In the absence of acid, the signal for the methine protons under the flexible quinoxaline flaps and under the diazaphthalimide appear at $\delta=5.95$ and 5.67 ppm, respectively. Upon addition of CF_3COOD, the resonance under the quinoxaline shifts upfield to $\delta=5.15$ ppm, whereas the other methine resonance remains virtually unchanged (Figure 9a). The entire spectrum at 0 and 9.4 M CF_3COOD is shown in Figure 14SI.

Figure 9b depicts the ^{1}H NMR resonance of cyclopentane (1.2 equiv) encapsulated in basket **1** (2.9×10^{-3} M) in [D_{12}]mesitylene. After the addition of CF_3COOD, the amount of encapsulated cyclopentane decreases drastically. At an acid concentration of 9.4 M, no more complexed guest is observed. Upon neutralization by means of extraction with aqueous K_2CO_3 solution, the bridged cavitand again becomes fully occupied by the guest (for the switching of tube **13**, see Figure 2SI).

Conclusion

Comprehensive host–guest complexation studies were performed with the resorcin[4]arene-based molecular basket **1** as a host and a broad variety of alicyclic and alicyclic heterocyclic guests. An X-ray crystal structure was obtained for **2**, a close analogue of **1**, and provided first crystallographic support for the postulated container-like structure in this family of synthetic receptors. Association constants (K_a) for the 1:1 complexes formed in mesitylene were measured with two different methods, ^{1}H NMR spectroscopy and ITC analysis. The K_a values at 303 K range from 1.7×10^2 M^{-1} for cycloheptane up to 1.7×10^7 M^{-1} for morpholine. In general, the heterocyclic guests form the more stable complexes. Six-membered-ring guests are much better encapsulated than most of the smaller- or larger-ring analogues. The measured differences in association constants, up to five orders of magnitude, can be explained by the steric fit of the guest molecules in the cavity and the additional interactions of the heterocyclic guests with the host. Optimal volume occupancy was investigated by molecular dynamics simulations, followed by volume calculations. The strongest complexation was observed at a PC of 63 ± 9%. Besides dispersion interactions and in particular C–H···π interactions between the encapsulated guest and the π surfaces in the walls, the capping bridge, and the resorcinarene bowl of the host, the best fitting heterocycles undergo additional polar interactions (C–O···C=O, N–H···π, and S···π) when bound to the cavity. This raises the PC beyond the value of 55 ± 9% observed for purely apolar complexation.[11] Preferred orientations of the heterocyclic guests in the cavity of cavitand **1** were identified by ROESY spectroscopy. Thermodynamic data from ITC analysis show that binding is driven by both a favorable enthalpic and entropic change. The latter is largest for the guests that are too small to fully fill the cavity. The enthalpic driving force is highest when additional polar interactions are established. Guest binding is reversibly switchable: upon addition of CF_3COOD, the quinoxaline flaps open up and the cargo is rapidly and quantitatively released from the host, whereas subsequent neutralization fully re-establishes guest encapsulation.

Experimental Section

Materials and general methods: See the Supporting Information. This section only includes the synthesis and characterization of the molecular baskets **1** and **2** and their side products, tubelike dimeric **11** and **13**; all other syntheses are reported in the Supporting Information. The naming of the compounds by the "phane nomenclature"[37] is also included in the Supporting Information.

Molecular basket 1 and tube 13: A suspension of tetrol **12** (1.00 g, 0.928 mmol) and tetrachloride **9** (649 mg, 1.21 mmol) in DMF (880 mL)

was treated dropwise with DIPEA (713 μL, 4.18 mmol). The solution was stirred at 85 °C for 18 h, cooled to 25 °C, and poured on ice-cold saturated aqueous NaCl solution (2 L). The yellow-orange suspension was stirred for 1 h. The mixture was extracted with CH_2Cl_2 (3×200 mL). The combined organic extracts were washed with saturated aqueous NaCl, dried over $MgSO_4$, and evaporated in vacuo. Medium-pressure liquid chromatography (MPLC; CH_2Cl_2/EtOAc 100:0 to 100:10 in 75 min, 50 mL min^{-1}) afforded **1** (317 mg, 23%) and **13** (133 mg, 10%) as off-white solids.

Basket 1: M.p. > 295 °C (decomp); ^{1}H NMR (400 MHz, $CDCl_3$, 298 K): δ = 0.90–0.94 (m, 12H), 1.31–1.50 (m, 32H), 2.19 (q, J = 7.6 Hz, 4H), 2.29 (q, J = 7.5 Hz, 4H), 4.60 (s, 4H), 5.53 (t, J = 8.2 Hz, 2H), 5.75 (t, J = 8.3 Hz, 2H), 6.81 (s, 4H), 7.20 (s, 4H), 7.89–7.93 (m, 4H), 8.20 (s, 4H), 8.28–8.32 ppm (m, 4H); ^{13}C NMR (100 MHz, $CDCl_3$, 298 K): δ = 14.19, 14.21, 22.79, 22.80, 28.04, 28.09, 29.43, 29.49, 31.90, 31.95, 32.05, 33.17, 34.04, 34.20, 41.31, 118.97, 123.64, 129.18, 129.70, 129.92, 135.44, 135.73, 136.99, 139.77, 141.95, 152.22, 152.59, 152.83, 158.21, 161.25 ppm; IR (neat): $\tilde{\nu}$ = 2925 (w), 1736 (m), 1481 (m), 1443 (w), 1411 (m), 1369 (s), 1329 (s), 1262 (m), 1220 (w), 1198 (s), 1157 (m), 1072 (m), 894 (m), 760 (m), 636 cm^{-1} (w); HR-MALDI-MS: *m/z* (%): calcd for $C_{88}H_{81}N_{10}O_{12}^+$: 1469.6030, found: 1469.6031 (56, $[M+H]^+$), 1470.6102 (100), 1471.6156 (70), 1472.6193 (33); elemental analysis calcd (%) for $C_{88}H_{80}N_{10}O_{12}$ (1469.66): C 71.92, H 5.49, N 9.53; found: C 71.44, H 5.68, N 9.48.

Tube 13: M.p. > 305 °C (decomp); ^{1}H NMR (400 MHz, $CDCl_3$, 298 K): δ = 0.90–0.96 (m, 24H), 1.33–1.51 (m, 64H), 2.24–2.32 (m, 16H), 4.92 (br s, 8H), 5.61 (br s, 4H), 5.71 (t, J = 8.2 Hz, 4H), 6.87 (br s, 4H), 7.01 (br s, 8H), 7.26 (s, 8H), 7.64 (br s, 4H), 7.89–7.93 (m, 4H), 8.01–8.05 (m, 4H), 8.24 ppm (br s, 8H), (no assignment of the signals was carried out due to very broad signals, high-temperature NMR measurements were carried out but no sharpening of the lines in the aromatic area was observed); ^{13}C NMR (100 MHz, $CDCl_3$, 298 K): δ = 14.05, 22.65, 27.95, 29.34, 31.86, 32.30, 32.66, 34.14, 41.09, 118.90, 123.72, 127.70, 128.18, 128.46, 129.25, 129.76, 135.68, 136.95, 139.78, 141.76, 152.04, 152.27, 153.07, 158.68, 162.27 ppm (5 signals are missing due to overlap or they are hidden in the noise. Due to conformational equilibria caused by the tilted phenyl bridge, signals are broadened); IR (neat): $\tilde{\nu}$ = 2926 (m), 2856 (w), 1790 (w), 1738 (s), 1580 (w), 1482 (m), 1445 (w), 1410 (s), 1372 (s), 1327 (s), 1261 (m), 1220 (m), 1200 (s), 1155 (s), 1117 (m), 1080 (m), 942 (w), 895 (m), 764 (s), 735 (m), 617 cm^{-1} (w); HR-MALDI-MS: *m/z* (%): calcd for $C_{176}H_{161}N_{20}O_{24}^+$: 2938.1987, found: 2938.2024 (43) $[M+H]^+$, 2939.1988 (89), 2490.1975 (100), 2941.2004 (81), 2942.2092 (49), 2943.2156 (24).

Molecular basket 2 and tube 11: A suspension of tetrol **8** (650 mg, 0.423 mmol) and tetrachloride **9** (251 mg, 0.465 mmol) in DMF (170 mL) was treated dropwise with Et_3N (265 μL, 1.90 mmol). The resulting solution was stirred at 70 °C for 18 h, cooled to 25 °C, and poured on ice-cold saturated aqueous NaCl solution (400 mL). The yellow-orange suspension was stirred for 1 h. The mixture was extracted with CH_2Cl_2 (2× 300 mL). The combined organic phases were washed with saturated aqueous NaCl solution, dried over $MgSO_4$, and evaporated in vacuo. The yellow solid was taken up in $CHCl_3$ and evaporated to dryness. The crude product was purified by flash chromatography (SiO_2; CH_2Cl_2/EtOAc 100:0 to 100:10 in 75 min, 50 mL min^{-1}) to afford monomeric **2** (51 mg, 6%) and dimeric **11** (77 mg, 9%) as colorless glasslike solids.

Basket 2: M.p. > 310 °C (decomp); ^{1}H NMR (400 MHz, $CDCl_3$, 298 K): δ = 1.27 (s, 36H), 1.28 (s, 36H), 3.60 (d, J = 8.2 Hz, 4H), 3.70 (d, J = 8.2 Hz, 4H), 4.60 (s, 4H), 6.13 (t, J = 8.2 Hz, 2H), 6.33 (t, J = 8.2 Hz, 2H), 6.82 (s, 4H), 7.07 (d, J = 1.7 Hz, 4H), 7.19 (d, J = 1.7 Hz, 4H), 7.21 (t, J = 1.7 Hz, 2H), 7.23 (t, J = 1.7 Hz, 2H), 7.54 (s, 4H), 7.91–7.93 (m, 4H), 8.20 (s, 4H), 8.29–8.32 ppm (m, 4H); ^{13}C NMR (100 MHz, $CDCl_3$, 298 K): δ = 31.64, 31.69, 34.59, 34.95, 34.97, 35.02, 38.11, 39.22, 41.33, 119.01, 120.48, 120.58, 122.85, 122.97, 124.32, 129.17, 129.77, 129.93, 135.45, 135.63, 136.91, 137.69, 137.89 139.78, 142.00, 150.83, 150.90, 152.22, 152.58, 152.80, 158.17, 161.21 ppm; IR (neat): $\tilde{\nu}$ = 2954 (m), 1738 (s), 1668 (w), 1599 (m), 1481 (m), 1443 (w), 1412 (s), 1363 (s), 1337 (s), 1265 (m), 1222 (m), 1199 (s), 1158 (s), 1074 (s), 1030 (w), 922 (m), 896 (m), 865 (m), 800 (w), 759 (s), 711 (m), 635 cm^{-1} (m); HR-MALDI-MS: *m/z* (%): calcd for $C_{124}H_{121}N_{10}O_{12}^+$: 1941.9160, found: 1941.9211 (54) $[M+H]^+$, 1942.9333 (100), 1943.9370 (78), 1944.9410 (46), 1945.9455 (23).

Tube 12: M.p. > 300 °C (decomp); ^{1}H NMR (400 MHz, $CDCl_3$, 298 K): δ = 1.29 (s, 144H), 3.68–3.75 (m, 16H), 4.92 (br s, 8H), 6.17 (br s, 4H), 6.32 (t, J = 8.2 Hz, 4H), 6.84 (br s, 4H), 7.01 (br s, 8H), 7.14 (s, 8H), 7.16 (d, J = 1.7 Hz, 8H), 7.23 (t, J = 1.7 Hz, 4H), 7.24 (t, J = 1.7 Hz, 4H), 7.61 (s, 8H), 7.64 (br s, 4H), 7.90–7.91 (m, 4H), 8.03–8.04 (m, 4H), 8.23–8.25 ppm (m, 8H); ^{13}C NMR (100 MHz, $CDCl_3$, 298 K): δ = 31.54, 34.68, 34.84, 38.44, 38.75, 41.10, 108.33, 118.94, 120.38, 120.46, 122.77, 211.79, 124.35, 127.68, 127.76, 134.70, 135.64, 136.71, 137.59, 137.63, 139.71, 141.71, 150.75, 151.99, 152.28, 153.08, 158.67, 162.45 ppm (4 signals are missing due to overlap or they are hidden in the noise. Due to conformational equilibria caused by the tilted phenyl bridge, signals are broadened); IR (neat): $\tilde{\nu}$ = 2954 (m), 1739 (m), 1598 (w), 1480 (m), 1446 (w), 1412 (m), 1372 (s), 1330 (s), 1248 (w), 1223 (w), 1200 (s), 1157 (m), 1064 (w), 1030 (w), 895 (m), 864 (m), 755 (s), 710 (m), 666 cm^{-1} (w); HR-MALDI-MS: *m/z* (%): calcd for $C_{248}H_{241}N_{20}O_{24}^+$: 3882.8253, found: 3882.8349 (31) $[M+H]^+$, 3883.8354 (69), 3884.8316 (99), 3885.8273 (100), 3886.8257 (79), 3887.8272 (55), 3888.8305 (31), 3889.8371 (13).

NMR binding studies: ^{1}H NMR studies were performed with a Bruker DRX 500 spectrometer. As solvent, specially purified [D_{12}]mesitylene from ARMAR, 99 Atom%D, was used. The purity was determined by GC/MS (see Figure 4SI).

For the experiments, which were done in double to quadruple runs, a stock solution of container molecule **1** in [D_{12}]mesitylene was prepared (about 3×10^{-3} M). A total of 0.6 equiv of 1,3,5-trimethoxybenzene in [D_{12}]mesitylene (about 2.5×10^{-2} M) as internal standard was added directly to the host stock solution. A total of 600 μL of host solution was transferred into new NMR tubes, and TMS was added.

Stock solutions of guests in [D_{12}]mesitylene were prepared (about 9×10^{-1} M) and added twice to the host solution (0.4 equiv and 0.8 equiv) during the measurement at 303 K.

The concentration of free and encapsulated guest was calculated from the peak area of the internal standard and the encapsulated guest, considering the corresponding number of protons and concentration of internal standard as well as the total amount of added guest. Finally, the K_a value was calculated according to $K_a = [HG]/[H]\times[G]$.

ITC analysis: ITC studies were performed using a commercial calorimeter MicroCal VP-ITC. As solvent, mesitylene from Acros, 99% extra pure, was used. The purity was determined by GC/MS (Figure 4SI).

For the experiments, which were done in double to pentuple runs, 25 portions of 10 μL of host solution (about 1×10^{-3} M to 4×10^{-3} M) were added to a solution of the guest (about 0.1×10^{-3} M) at intervals of 240 s with the first addition being only 2 μL. The power P that was needed to keep the sample at 30 °C was monitored over time t. The heat of dilution for the addition of host solution to pure mesitylene was measured for all used concentrations and subtracted. The heat of dilution for the addition of pure mesitylene into guest solution was measured as well. The measured values were too small for an evaluation and were neglected.

For evaluation of the data, the area of the peaks in the P/t diagram were evaluated with Origin 7,[38] and the heat of dilution was subtracted. The resulting sets of data points were then fitted with Origin 7 giving access to the thermodynamic data and K_a values that are summarized in Table 1.

MD calculations: MD calculations were performed using MacroModel 9.7 (molecular dynamics, OPLS 2005 force field, 300 K, Δt = 1.5 fs, simulation time 1000 ps).

X-ray analysis: Compound **2**, $C_{124}H_{120}N_{10}O_{12}\times CH_2Cl_2$, M_r = 2027.27. A crystal of the size 0.33×0.27×0.14 mm was measured at 123 K on a Bruker-Nonius Kappa-CCD with $Mo_{K\alpha}$ radiation, λ = 0.71073 Å. Monoclinic space group $P2_1$, ρ_{calcd} = 1.084 g cm^{-3}, Z = 2, a = 14.2720(6) Å, b = 24.8574(11) Å, c = 18.3511(9) Å, β = 108.598(2)°, V = 6170.4(5) Å^3, μ = 0.156 mm^{-1}. Of the 18110 measured reflexions 13066 were independent (R_{int} = 0.08). The structure was solved by direct methods (SHELXS-97),[39] and refined by full-matrix least-squares analysis (SHELXL-97).[39] Heavily disordered structure with space group ambiguity. Solved and refined in several space groups (orthorhombic C-centered, monoclinic $P2_1/m$ and $P2_1$) Best result in $P2_1$. Possible multiple twin (ca. 60:20:20). Structure solution depicts the well-defined cage, two complete diisopropyl-

phenyl fragments and part of a third one. The fourth substituent had to be constructed completely. All substituents were included in the refinement as rigid body allowing the isopropyl groups to rotate. Two Cl atoms have been assigned to two electron peaks in the cavity assuming a CH_2Cl_2 molecule with totally disordered C atom (not included). Final $R(F)=0.324$, $wR(F^2)=0.642$ for 10165 reflections with $I>2\sigma(I)$.

CCDC 797074 contains the supplementary crystallographic data for this paper. These data can be obtained free of charge from The Cambridge Crystallographic Data Centre via www.ccdc.cam.ac.uk/data_request/cif.

Acknowledgements

This work was supported by the European Union through the Marie-Curie Research Training Network PRAIRIES, contract MRTN-CT-2006–035810, the Swiss National Science Foundation, and the NCCR "Nanoscale Science". L.D.S. acknowledges a NSF-IRFP postdoctoral fellowship from the US National Science Foundation. We thank Dr. M.-O. Ebert (ETH) for assistance with NMR spectroscopy, P. Kälin (ETH) for guidance with the ITC measurements, and A. Dutly (ETH) for help with GC/MS measurements. Prof. Gerhard Klebe (Universität Marburg) is acknowledged for discussions about limitations of van't Hoff plot analysis.

[1] T. Gottschalk, B. Jaun, F. Diederich, *Angew. Chem.* **2006**, *119*, 264–268; *Angew. Chem. Int. Ed.* **2007**, *46*, 260–264.
[2] T. Gottschalk, P. D. Jarowski, F. Diederich, *Tetrahedron* **2008**, *64*, 8307–8317.
[3] J. R. Moran, S. Karbach, D. J. Cram, *J. Am. Chem. Soc.* **1982**, *104*, 5826–5828.
[4] D. J. Cram, J. M. Cram, *Container Molecules and Their Guests*, The Royal Society of Chemistry, Cambridge, **1997**.
[5] E. Dalcanale, P. Soncini, G. Bacchilega, F. Ugozzoli, *J. Chem. Soc. Chem., Commun.* **1989**, 500–502.
[6] S. Zampolli, P. Betti, I. Elmi, E. Dalcanale, *Chem. Commun.* **2007**, 2790–2792.
[7] V. A. Azov, B. Jaun, F. Diederich, *Helv. Chim. Acta* **2004**, *87*, 449–462.
[8] R. J. Hooley, H. Van Anda, J. Rebek, Jr., *J. Am. Chem. Soc.* **2006**, *128*, 3894–3895.
[9] E. Mann, J. Rebek, Jr., *Tetrahedron* **2008**, *64*, 8484–8487.
[10] L. D. Shirtcliff, H. Xu, F. Diederich, *Eur. J. Org. Chem.* **2010**, 846–855.
[11] S. Mecozzi, J. Rebek, Jr., *Chem. Eur. J.* **1998**, *4*, 1016–1022.
[12] M. Yoshifuji, K. Shimura, K. Toyota, *Bull. Chem. Soc. Jpn.* **1994**, *67*, 1980–1983.
[13] V. A. Azov, P. J. Skinner, Y. Yamakoshi, P. Seiler, V. Gramlich, F. Diederich, *Helv. Chim. Acta* **2003**, *86*, 3648–3670.
[14] M. J. Plater, S. Aiken, G. Bourhill, *Tetrahedron* **2002**, *58*, 2405–2413.
[15] P. J. Skinner, A. G. Cheetham, A. Beeby, V. Gramlich, F. Diederich, *Helv. Chim. Acta* **2001**, *84*, 2146–2153.
[16] M. G. J. Beets, W. Meerburg, H. Vanessen, *Recl. Trav. Chim. Pays-Bas* **1959**, *78*, 570–585.
[17] V. A. Azov, F. Diederich, Y. Lill, B. Hecht, *Helv. Chim. Acta* **2003**, *86*, 2149–2155.
[18] P. P. Castro, G. Zhao, G. A. Masangkay, C. Hernandez, L. M. Gutierrez-Tunstad, *Org. Lett.* **2004**, *6*, 333–336.
[19] Spartan'08, Macintosh Version 1.0.3, Wavefunction Inc., 18401 Von Karman Ave., Irvine, **2008**.
[20] T. Heinz, D. M. Rudkevich, J. Rebek, Jr., *Nature* **1998**, *394*, 764–766.
[21] P. Roncucci, L. Pirondini, G. Paderni, C. Massera, E. Dalcanale, V. A. Azov, F. Diederich, *Chem. Eur. J.* **2006**, *12*, 4775–4784.
[22] L. Fielding, *Tetrahedron* **2000**, *56*, 6151–6170.
[23] J. L. Sessler, D. E. Gross, W.-S. Cho, V. M. Lynch, F. P. Schmidtchen, G. W. Bates, M. E. Light, P. A. Gale, *J. Am. Chem. Soc.* **2006**, *128*, 12281–12288.
[24] For ITC measurements on cavitands, see: a) F. Tancini, R. M. Yebeutchou, L. Pirondini, R. De Zorzi, S. Geremia, O. A. Scherman, E. Dalcanale, *Chem. Eur. J.* **2010**, *16*, 14313–14321; b) F. Tancini, T. Gottschalk, W. B. Schweizer, F. Diederich, E. Dalcanale, *Chem. Eur. J.* **2010**, *16*, 7813–7819; c) H. Gan, B. C. Gibb, *Supramol. Chem.* **2010**, *22*, 808–814.
[25] F. Diederich, K. Dick, D. Griebel, *Chem. Ber.* **1985**, *118*, 3588–3619.
[26] E. Freire, *Drug Discovery Today* **2008**, *13*, 869–874.
[27] For polar effects in the complexation of adamantyl derivatives in rim-functionalized open cavitands, see: R. J. Hooley, S. R. Shenoy, J. Rebek, Jr., *Org. Lett.* **2008**, *10*, 5397–5400.
[28] R. Paulini, K. Müller, F. Diederich, *Angew. Chem.* **2005**, *117*, 1820–1839; *Angew. Chem. Int. Ed.* **2005**, *44*, 1788–1805.
[29] C. Allott, H. Adams, P. L. Bernad, Jr., C. A. Hunter, C. Rotger, J. A. Thomas, *Chem. Commun.* **1998**, 2449–2450.
[30] For reviews on interactions with aromatic rings, see: a) E. A. Meyer, R. K. Castellano, F. Diederich, *Angew. Chem.* **2003**, *115*, 1244–1287; *Angew. Chem. Int. Ed.* **2003**, *42*, 1210–1250; b) L. M. Salonen, M. Ellermann, F. Diederich, *Angew. Chem.* **2011**, *123*, 4908–4944; *Angew. Chem. Int. Ed.* **2011**, *50*, 4808–4842.
[31] For other reviews on the mechanisms of molecular recognition, see: a) I. K. Mati, S. L. Cockroft, *Chem. Soc. Rev.* **2010**, *39*, 4195–4205; b) H.-J. Schneider, *Angew. Chem.* **2009**, *121*, 3982–4036; *Angew. Chem. Int. Ed.* **2009**, *48*, 3924–3977.
[32] MacroModel, Version 9.7, Schrödinger LLC, New York, **2009**.
[33] G. J. Kleywegt, VOIDOO, version 3.3.4, Uppsala Software Factory, Uppsala, **2007**.
[34] T. Gottschalk, Dissertation, Eidgenössische Technische Hochschule Zürich (Switzerland), **2008**, Number 18067.
[35] L. Pirondini, D. Bonifazi, B. Cantadori, P. Braiuca, M. Campagnolo, R. De Zorzi, S. Geremia, F. Diederich, E. Dalcanale, *Tetrahedron* **2006**, *62*, 2008–2015.
[36] M. Zürcher, T. Gottschalk, S. Meyer, D. Bur, F. Diederich, *ChemMedChem* **2008**, *3*, 237–240.
[37] H. A. Favre, D. Hellwinkel, W. H. Powell, H. A. Smith, Jr., S. S.-C. Tsay, *Pure Appl. Chem.* **2002**, *74*, 809–834.
[38] Origin 7, OriginLab Corporation, Northampton, **2002**.
[39] G. M. Sheldrick, *Acta Crystallogr. A* **2008**, *64*, 112–122.

Received: June 17, 2011
Published online: September 21, 2011

